Intranucleolar sites of ribosome biogenesis defined by the localization of early binding ribosomal proteins

Tim Krüger,[1] Hanswalter Zentgraf,[2] and Ulrich Scheer[1]

[1]Department of Cell and Developmental Biology, Biocenter, University of Würzburg, D-97074 Würzburg, Germany
[2]Department of Tumor Virology, German Cancer Research Center, D-69120 Heidelberg, Germany

Considerable efforts are being undertaken to elucidate the processes of ribosome biogenesis. Although various preribosomal RNP complexes have been isolated and molecularly characterized, the order of ribosomal protein (r-protein) addition to the emerging ribosome subunits is largely unknown. Furthermore, the correlation between the ribosome assembly pathway and the structural organization of the dedicated ribosome factory, the nucleolus, is not well established. We have analyzed the nucleolar localization of several early binding r-proteins in human cells, applying various methods, including live-cell imaging and electron microscopy. We have located all examined r-proteins (S4, S6, S7, S9, S14, and L4) in the granular component (GC), which is the nucleolar region where later pre-ribosomal RNA (rRNA) processing steps take place. These results imply that early binding r-proteins do not assemble with nascent pre-rRNA transcripts in the dense fibrillar component (DFC), as is generally believed, and provide a link between r-protein assembly and the emergence of distinct granules at the DFC–GC interface.

Introduction

Progress in functional proteomics of the nucleolus and nucleolar protein complexes has begun to reveal the complex pathway of eukaryotic ribosome biogenesis. Advances in affinity purification methods and mass spectrometry have allowed the identification of several multiprotein complexes containing hundreds of proteins involved in the production of nucleolar preribosomes. Integration of these results by bioinformatical approaches have led to a tentative map of ribosome assembly pathways (Fromont-Racine et al., 2003; Milkereit et al., 2003; Hinsby et al., 2006). However, ribosomal proteins (r-proteins) were largely excluded from such analyses because of their tendency to bind nonspecifically to isolated protein complexes (Milkereit et al., 2003). Based on previous seminal biochemical analyses of early and late stage preribosomes isolated from mammalian and yeast nucleoli, it is generally assumed that a distinct set of r-proteins (the early assembly group) binds to the pre-ribosomal RNA (rRNA) during or immediately after transcription (Hadjiolov, 1985; Fromont-Racine et al., 2003; de la Cruz et al., 2004; Gerbi and Borovjagin, 2004). This notion received further support from an immunoelectron microscopic study of spread rRNA genes ("Christmas trees") of *Drosophila melanogaster* showing the direct association of the r-proteins S14 and L4 with the growing pre-rRNA fibrils (Chooi and Leiby, 1981). More recently, five r-proteins (S4, S6, S7, S9, and S14) were identified by proteomic analyses as integral components of the small subunit (SSU) processome of yeast (Bernstein et al., 2004; a similar RNP complex was identified and termed 90S particle by Grandi et al. [2002]). The SSU processome is an RNP particle that is thought to correspond to the large electron-dense terminal knobs seen in electron microscopic spreads of yeast chromatin at the free (5′) ends of nascent pre-rRNA transcripts (Osheim et al., 2004). Hence, the SSU processome–associated r-proteins can be classified as early binding proteins. In fact, three of them (S4, S6, and S14) belong to the early assembly group identified in mammalian cells, as does L4, although it is absent from the SSU processome (Hadjiolov, 1985).

The process of ribosome biogenesis can be spatially subdivided and assigned to different nucleolar compartments. Nucleoli contain three morphologically distinct components,

Correspondence to Ulrich Scheer: scheer@biozentrum.uni-wuerzburg.de

Abbreviations used in this paper: AMD, actinomycin D; DFC, dense fibrillar component; DRB, 5,6-dichloro-1-β-D-ribofuranosylbenzimidazole; FC, fibrillar center; GC, granular component; mRFP, monomeric red fluorescent protein; NOR, nucleolus organizing region; r-protein, ribosomal protein; rRNA, ribosomal RNA; snoRNP, small nucleolar RNP; SSU processome, small subunit processome.

The online version of this article contains supplemental material.

The Journal of Cell Biology, Vol. 177, No. 4, May 21, 2007 573–578
http://www.jcb.org/cgi/doi/10.1083/jcb.200612048

which reflect the vectorial process of ribosome production. Synthesis, modification, and initial cleavage steps of the pre-rRNA take place within the fibrillar components (fibrillar center [FC] and the surrounding dense fibrillar component [DFC]), whereas later processing steps are performed in the granular component (GC; for review see Huang, 2002). It is generally assumed that preribosome assembly begins in the DFC of mammalian cells with the formation of 80S RNP complexes containing full-length pre-rRNAs, early binding r-proteins, and numerous nonribosomal proteins and processing and assembly factors (Royal and Simard, 1975; Hadjiolov, 1985; Gerbi and Borovjagin, 2004). A similar scheme applies for yeast (Kruiswijk et al., 1978; Gadal et al., 2002), albeit the occurrence of co-transcriptional processing events in these cells has complicated the identification of primary preribosomes containing the full-length RNA transcript (Granneman and Baserga, 2004).

The notion that 80S preribosomes are assembled in the DFC was recently challenged by a study that analyzed the spatial distribution of several preribosome-associated nonribosomal proteins (Leary et al., 2004). The authors proposed that the most likely site of integration of proteins such as Imp3, Imp4, and Mpp10 into the emerging SSU processome is not the DFC but rather the DFC–GC interface of mammalian nucleoli (for a detailed characterization of the human SSU processome, see Granneman et al. [2003]). We have used similar cell biological approaches to clarify the intranucleolar localization of all r-proteins considered early binding and to examine the question of whether they actually accompany the pre-rRNAs on their intranucleolar pathway from the very beginning, as suggested by biochemical analyses.

Results and discussion

We have cloned cDNAs coding for the early binding human r-proteins S4, S6, S7, S9, S14, and L4. In addition, we have raised antibodies against recombinant S14 to examine the distribution of endogenous S14. The r-proteins were transiently expressed as GFP fusion proteins in Hep2 cells with GFP fused to either the N or the C terminus. To address potential localization problems caused by GFP, because of sterical hindrance or the duration of GFP maturation, the proteins were also fused to a fast maturing YFP (Venus; Nagai et al., 2002) and to a short myc tag that was detected by immunofluorescence. With the appropriate tag, all chimeric r-proteins displayed an intracellular distribution consistent with the well-known fact that ribosomal subunits are assembled in nucleoli and then exported to the cytoplasm (Fig. 1, a–h). The GFP fusion proteins S4, S6, S9, S14, and L4 (GFP C-terminal), as well as the corresponding Venus fusions and the myc-tagged proteins S7, S9, S14, and L4 (myc N-terminal), localized in the nucleolus and the cytoplasm, with very little detectable signal in the nucleoplasm. None of the N-terminal GFP fusion proteins localized correctly, either not being directed to the nucleolus or not being exported to the cytoplasm. To verify that the distribution of the expressed fusion proteins mirrored

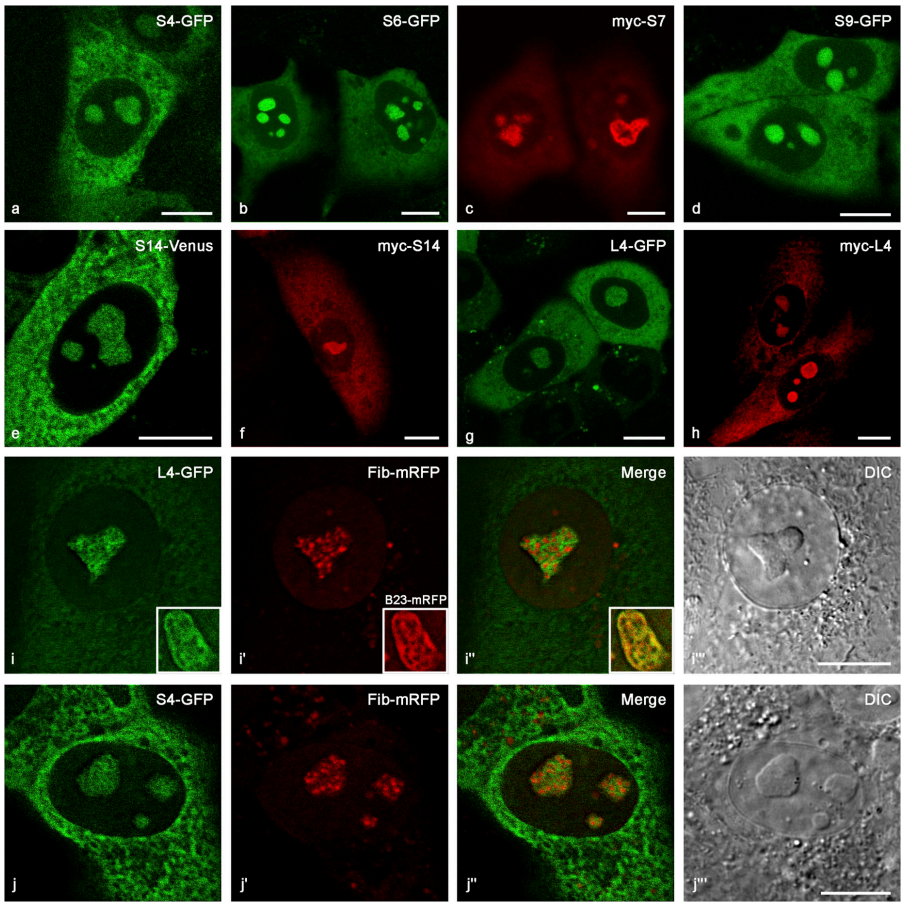

Figure 1. **Localization of early binding r-proteins in human Hep2 cells by confocal microscopy after transient expression as fusions with fluorescent proteins or with a myc epitope.** (a–h) The distribution of r-proteins fused to GFP or the rapidly maturing spectral variant Venus is shown in living cells, whereas myc-tagged r-proteins were visualized by immunofluorescence of fixed cells with anti-myc antibodies. Note the characteristic distribution pattern of all expressed r-proteins, which are concentrated in the nucleoli, almost absent from the nucleoplasm, and dispersed throughout the cytoplasm. (rows i and j) L4 and S4 do not colocalize with mRFP-tagged fibrillarin, a marker of the DFC of the nucleolus, as revealed by double expression in live Hep2 cells. Note that the fibrillarin-positive structures (i′ and j′) correspond to regions deficient of r-proteins (i and j; the merged images are shown in i″ and j″). In contrast, L4-GFP colocalizes with B23-mRFP, which marks the GC (row i, insets). Corresponding differential interference contrast (DIC) images are also shown. Bars, 10 μm.

that of their endogenous counterparts, we exemplarily raised an antibody against recombinant S14. In immunoblots of isolated cytoplasmic ribosomal subunits, the antibody (mAb S14-39) recognized a protein of 15 kD of the small (40S) subunit (Fig. 2 b; calculated M_r of S14 = 16,273). When probed by immunofluorescence, the antibodies labeled nucleoli and the cytoplasm (Fig. 2 a) in a pattern comparable to that produced by the expression of Venus-tagged S14 (Fig. 1 e). The characteristic nucleolar/cytoplasmic distribution pattern was also seen in a stably transfected Hep2 cell line expressing S4-GFP (unpublished data). As judged from the growth and division of the transfected cells, the tagged r-proteins did not interfere with basic cellular processes. To prove that S4-GFP was actually incorporated into cytoplasmic ribosomes, we isolated ribosomal subunits from the cell line followed by SDS-PAGE and immunoblotting experiments with antibodies against GFP. As shown in Fig. 2 c, the antibodies recognized a polypeptide band of the small (40S) but not of the large (60S) ribosomal subunits with an apparent molecular mass of ~55 kD, in agreement with the combined molecular masses of S4 (30 kD) and GFP (27 kD).

To correlate the distribution of r-proteins with specific nucleolar components in living cells, we simultaneously expressed fibrillarin fused to monomeric red fluorescent protein (Fib-mRFP) and an r-protein fused to GFP. Fibrillarin is an established marker protein of the DFC of the nucleolus. High-resolution confocal microscopy revealed a clear topological separation between fibrillarin and all examined r-proteins, as shown for L4 and S4 (Fig. 1, rows i and j). The r-proteins appeared to fill the space between the fibrillarin-positive structures, which corresponds to the GC. The assignment of the r-proteins to the GC of the nucleolus was further confirmed by their colocalization with B23-mRFP, an established marker of the GC (Fig. 1, row i, insets).

Treatment of cells with low doses of actinomycin D (AMD) inhibits RNA polymerase I–mediated transcription and causes the visible segregation of nucleolar components into closely apposed yet distinct structural entities (Leary et al., 2004). None of the r-proteins colocalized with the marker protein fibrillarin in the segregated DFC, which formed cap-like structures apposed to the GC. Instead, as shown exemplarily for endogenous S14 and S6-GFP, the r-proteins were located in the larger and almost spherical component adjacent to the DFC (Fig. 3, rows a and b). The identity of this component as the GC was ascertained by coexpression of tagged marker proteins for the DFC (fibrillarin-RFP) and the GC (B23-GFP; Fig. 3 a″, inset). Furthermore, the distribution of the r-proteins coincided with B23 after treatment of cells with low doses of AMD (unpublished data).

It is a distinct possibility that upon AMD treatment the previously synthesized RNA molecules including prematurely

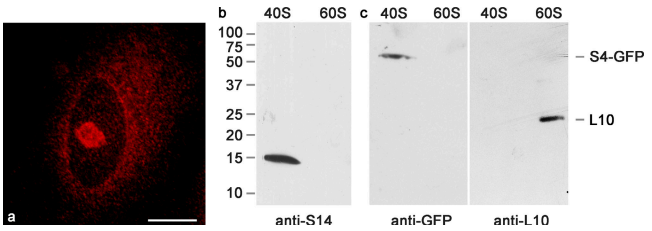

Figure 2. **Characterization of mAb S14-39 raised against recombinant S14.** (a) The antibodies stain the nucleolus and the cytoplasm of Hep2 cells. (b) In immunoblots, the mAb recognizes a 15-kD polypeptide of the small (40S) ribosomal subunit. (c) Incorporation of S4-GFP into cytoplasmic ribosomes. Ribosomes were isolated from a cell line stably expressing S4-GFP, and the subunits were analyzed by SDS-PAGE. Antibodies against GFP recognize an ~55-kD band of the small subunit, the expected molecular mass of the fusion protein (left). The separation of small and large ribosomal subunits was monitored with antibodies to L10 (right). Bar, 10 μm.

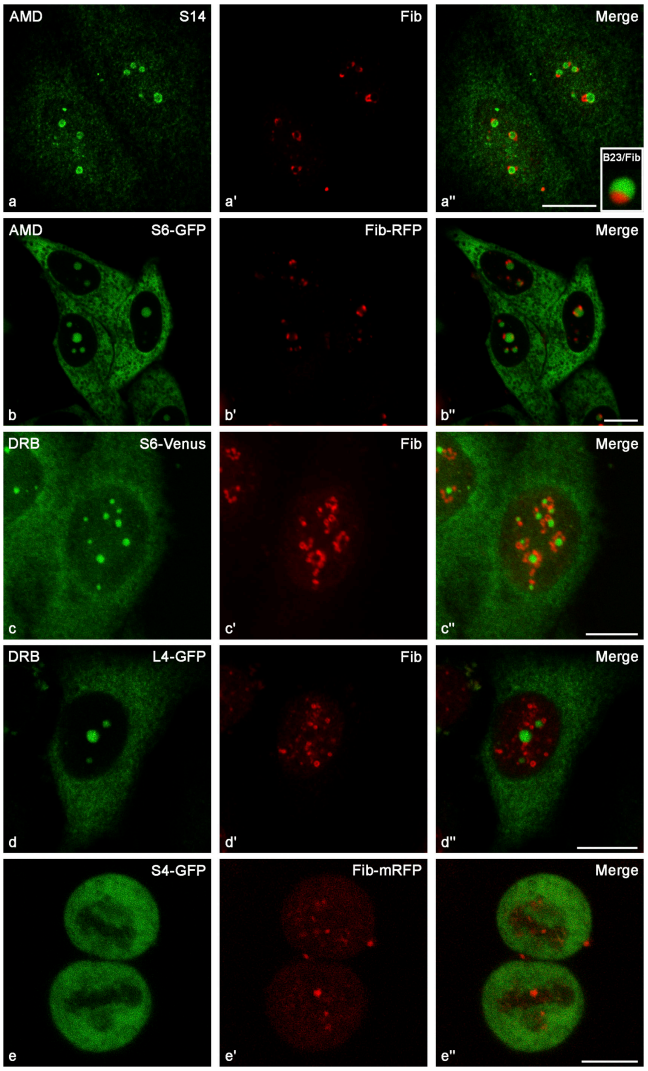

Figure 3. **Early binding r-proteins are restricted to the GC and absent from the DFC of nucleoli.** After AMD treatment, the two major nucleolar components, GC and DFC, segregate into separate structures (a″, inset; coexpression of the GC marker B23-GFP and the DFC marker fibrillarin-RFP). Endogenous S14 is absent from the DFC, stained with antibodies to fibrillarin (a–a″). S6-GFP is also absent from the DFC, marked by expression of fibrillarin-RFP in living cells (b–b″). DRB causes the unraveling of nucleoli into DFC (stained with antibodies to fibrillarin; c′ and d′) and spherical GC remnants. S6 and L4 are associated exclusively with these GC structures (c and d; merged images in c″ and d″). (e–e″) Localization of S4-GFP and fibrillarin-mRFP in a live mitotic Hep2 cell undergoing nucleolar reformation. Shown is a telophase ~20 min after the onset of anaphase. Reformation of the DFC around the chromosomal NORs occurs in the absence of S4. Around 10 min later, S4 begins to accumulate at the NORs, concurrent with the formation of the GC. Bars, 10 μm.

released transcripts migrate from the DFC into the GC, where they accumulate (Puvion-Dutilleul et al., 1997). Therefore, the absence of r-proteins from the DFC in AMD-treated cells could simply reflect the depletion of preribosomes from the DFC and not the inability of r-proteins to bind to early pre-rRNAs. To circumvent the interpretive problems inherent in the AMD experiments, we have exposed cells to the casein kinase 2 inhibitor 5,6-dichloro-1-β-D-ribofuranosylbenzimidazole (DRB), which does not inhibit transcription of the rRNA genes but causes the unraveling of nucleoli, along with the physical separation of the fibrillar components (FC/DFC) from the GC (Louvet et al., 2005). When cells expressing GFP- or Venus-tagged r-proteins were treated with DRB and counterstained with antibodies against fibrillarin to mark the DFC, the r-proteins were absent from the DFC, which often formed necklace-like structures, but were present in spherical GC remnants distributed throughout the nucleoplasm (Fig. 3, rows c and d). In independent experiments, we have confirmed the GC origin of the spherical masses based on the presence of B23 (unpublished data).

Nucleoli disintegrate during mitosis of mammalian cells. Reassembly is a stepwise process beginning with the formation of the DFC at the chromosomal nucleolus organizing regions (NORs), followed by the emergence of the GC. Kinetic analyses have shown that the DFC marker fibrillarin accumulates at the NORs several minutes before GC markers (Leung et al., 2004). When we performed live-cell microscopy with cells expressing S4-GFP and fibrillarin-mRFP, we observed a corresponding delay between the early recruitment of fibrillarin and of S4 at the NORs (Fig. 3, row e). On the other hand, the reassembly kinetics of S4 were comparable to that of B23 (unpublished data). We conclude that, during postmitotic nucleologenesis, S4 behaves like a bona fide component of the GC.

Next, we examined the intranucleolar localization of myc-tagged r-proteins and endogenous S14 by immunogold electron microscopy. We used pre- and postembedding labeling protocols, as both approaches have different assets and drawbacks. Irrespective of the method used or of the specific r-protein examined, the results were essentially identical. All the early binding r-proteins localized throughout the GC but were not detectable in the FC/DFC regions (for S9, S14, and L4 examples, see Fig. 4). The apparent absence of r-proteins from FC and DFC was not a consequence of limited antibody accessibility. This was shown by the effective decoration of the DFC with antibodies against fibrillarin (Fig. 4 f) and of the FC with antibodies against RNA polymerase I, an established marker of the FC (Fig. 4 g).

Notably, the localization of early binding r-proteins described in this study resembles the intranucleolar distribution of several nonribosomal proteins, which are integral components of the 80S preribosome (Leary et al., 2004). To compare the distribution of both protein classes directly, we have coexpressed one of the nonribosomal proteins, Imp3, together with either the r-protein S4 or the DFC marker fibrillarin using different fluorescent tags (Fig. S1, available at http://www.jcb.org/cgi/content/full/jcb.200612048/DC1). GFP-Imp3 was largely excluded from the DFC, in agreement with previously published data (Leary et al., 2004). In contrast, GFP-Imp3 and S4-Venus

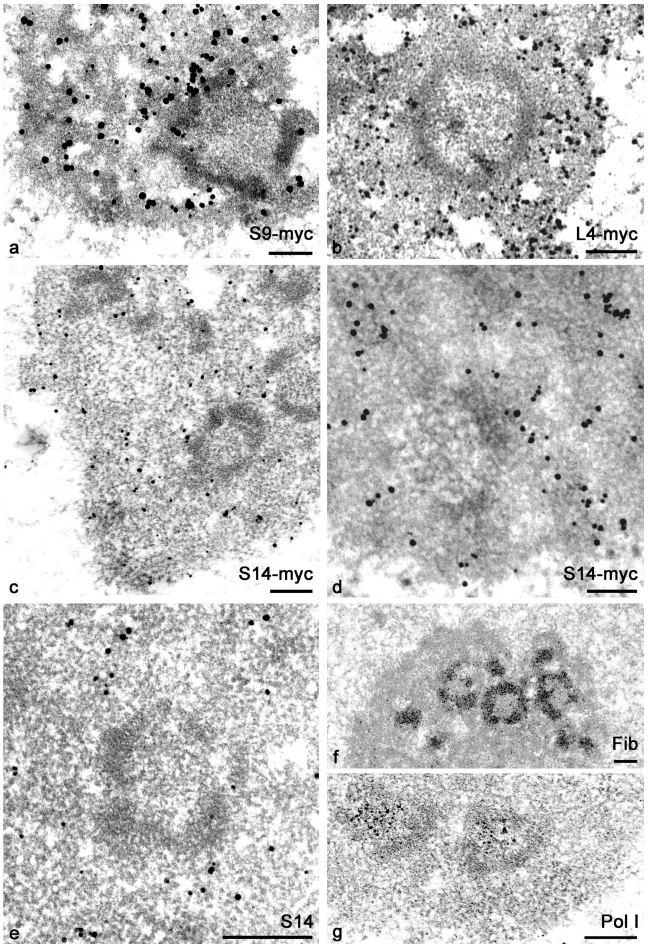

Figure 4. **Immunogold electron microscopy showing the intranucleolar distribution of early binding r-proteins in Hep2 cells.** FCs with the surrounding electron-dense DFC layer are clearly identified in all figures. Silver-enhanced gold particles are dispersed throughout the GC but are excluded from the DFC–FC complex. Myc-tagged S9, S14, and L4 were expressed in Hep2 cells and visualized using preembedding (b and c) or postembedding (a and d) labeling protocols followed by silver enhancement of the ultrasmall gold particles. Endogenous S14 was detected with mAb S14-39 (preembedding protocol; e). The DFC is accessible to antibodies, as illustrated by its strong labeling with antibodies to fibrillarin (mAb 72B9, preembedding protocol; f). Note that in this specific case, the silver enhancement reaction has been deliberately increased for optimized display of the signal in this survey image. The FCs are labeled with antibodies against RNA polymerase I (g). Bars, 0.2 μm.

colocalized extensively in the GC of nucleoli. Interestingly, the outermost regions of the GC contained relatively low concentrations of Imp3 as compared with S4, suggesting that the removal of nonribosomal protein and final maturation steps of ribosomal particles are confined to more peripheral regions of nucleoli.

Collectively, our results are difficult to reconcile with the generally held view that early binding r-proteins associate with pre-rRNAs during or immediately after transcription. If this were the case, the r-proteins should be readily detectable in the DFC, where both elongating and full-length primary transcripts are present at relatively high concentrations, as shown by in situ hybridization studies at the light and electron microscopic level (Puvion-Dutilleul et al., 1991, 1997; Lazdins et al., 1997). Rather, our data provide evidence that r-proteins do not assemble into

preribosomes until pre-rRNAs migrate from the DFC to the GC. In this aspect, our results substantiate the model of preribosome formation at the DFC–GC border proposed by Leary et al. (2004). It will be interesting to find out whether this step corresponds to a specific pre-rRNA cleavage event. In any event, our finding that r-proteins are first detectable in the GC, but that early processing events at both ends of the pre-rRNA already occur within the DFC (Lazdins et al., 1997; note that 3′ processing requires template-released pre-rRNAs), makes it unlikely, at least in human cells, that the r-proteins associate cotranscriptionally with elongating pre-rRNA transcripts, as has been concluded from electron microscopic immunolocalizations on Miller-type chromatin spreads (Chooi and Leiby, 1981).

However, at the moment we cannot exclude the formal possibility that the free ends of nascent pre-rRNA transcripts are the sites where assembly of preribosomes takes place, as suggested by Leary et al. (2004), similar to the situation described in yeast (Osheim et al., 2004). If this were the case, the nascent transcript fibrils of the rDNA transcription units must all be orientated toward the GC with their free ends aligned at the DFC–GC boundary. At the moment, virtually nothing is known about the spatial arrangement, compaction, and orientation of the rDNA transcription units in nucleoli of live mammalian cells. Furthermore, a structural correlate to the large (~35–45 nm) terminal yeast knob presumed to represent a fully assembled SSU processome has not yet been identified in chromatin spreads of higher eukaryotic cells (Osheim et al., 2004).

The abrupt appearance of granules at the DFC–GC interface is indicative of profound structural rearrangements of the nascent ribosomes. We propose that it is the binding of r-proteins that assists and stabilizes the correct folding of the rRNA (Fromont-Racine et al., 2003; Favaretto et al., 2005) and is thus causally involved in the transition from a more extended to a granular character of the preribosomes. What mechanisms might prevent the recruitment of r-proteins to early pre-rRNAs in the DFC, which spend ~20 min in this compartment before they appear in the GC (Thiry et al., 2000; Leung et al., 2004)? We envisage that the association of the large number of small nucleolar RNPs (snoRNPs) with the nascent transcripts competes with the binding of r-proteins. Two classes of snoRNPs mediate the site-specific 2-*O*-methylation and the isomerization of uridines to pseudouridines of the rRNAs (for review see Decatur and Fournier, 2003). During or immediately after synthesis, the primary pre-rRNA transcripts are modified by transient interactions with ~200 different snoRNA–protein complexes with methyltransferase (box C/D snoRNPs) or pseudouridylase (box H/ACA snoRNPs) activities. Each modification-guide RNA is associated with a specific set of proteins, and it is reasonable to assume that binding of numerous snoRNPs of considerable size not only prevents folding of the pre-rRNA (El Hage and Tollervey, 2004) but also prevents interactions with r-proteins.

The majority of snoRNPs are located in the DFC, as shown by the intranucleolar distribution of their core proteins and by in situ hybridization experiments with probes complementary to snoRNAs (Matera et al., 1994; Pogacic et al., 2000; Leary et al., 2004; Meier, 2005). It has been proposed that, upon snoRNP dissociation, the pre-rRNAs are extensively refolded by energy-requiring processes mediated by a plethora of transacting protein factors (El Hage and Tollervey, 2004). Our data suggest that r-proteins are involved in these structural rearrangements and that the actual assembly of ribosome subunits in human cells, i.e., the association of r-proteins with pre-rRNAs, occurs in the GC and is spatially separate from the sites of synthesis, chemical modification, and early processing of the pre-rRNA in the DFC.

It has proven difficult to deduce from the results of biochemical analyses alone the order of early assembly steps that lead to preribosomes in yeast and even more so in higher eukaryotes. In situ and in vivo analyses of the spatial distribution of specific preribosome-associated factors will be an important complement in defining pathways of ribosome assembly.

Materials and methods

cDNA, plasmids, and transfection

The following cDNAs were cloned by RT-PCR using total RNA isolated from Hep2 cells: S4 (gi:39812410), S6 (gi:20381195), S7 (gi:15431308), S9 (gi:550022), S14 (gi:14141191), L4 (gi:16579884), fibrillarin (gi:14763877), B23 (gi: 12803184), and Imp3 (gi:70908369). The cDNAs were cloned into the pCR2.1-Topo vector (Invitrogen), sequenced, and subcloned into the following vectors: pEGFP-N1, pEGFP-C1 or -C3, pDsRed-Monomer-N1, pCMV-Myc (all obtained from CLONTECH Laboratories, Inc.), pQ-C-His, and pVenus. pVenus was produced by site-directed mutagenesis of pEYFP (CLONTECH Laboratories, Inc.) as described by Nagai et al. (2002). Transfections were performed using Effectene (QIAGEN) or Fugene (Roche) according to the manufacturers' instructions. Transiently transfected cells were analyzed 24–72 h after transfection. The clone of Hep2 cells stably expressing S4-GFP was isolated after a 3-wk selection period with 0.75 mg/ml G418.

Antibodies

Hybridoma supernatant S14-39 was raised against His-tagged S14. S14-His fusion protein was expressed from the vector pQ-C-His in *Escherichia coli* XLI-blue and purified using Talon metal affinity resin (BD Biosciences). Further antibodies used were mAb 72B9 against fibrillarin (Reimer et al., 1987a), autoimmune serum S18 against pol I (Reimer et al., 1987b), anti-GFP (Sigma-Aldrich), c-Myc mAb (BD Biosciences), and QM (C-17) against L10 (Santa Cruz Biotechnology, Inc.).

Indirect immunofluorescence and live-cell microscopy

Hep2 cells grown on coverslips were fixed with 2% formaldehyde in PBS and permeabilized with 0.2% Triton X-100 in PBS and incubated for 30 min with the primary antibodies and 15 min with the appropriate Texas red–conjugated secondary antibodies (Dianova). In some experiments, cells were treated with 0.04 μg/ml AMD for 2–3 h or with 50 μg/ml DRB for 5–6 h before fixation or live-cell imaging. For live-cell microscopy, cells were grown on glass-bottomed dishes (WPI). Images were taken with a confocal laser-scanning microscope (TCS-SP or TCS-SP2; Leica) equipped with 63×/1.4 NA oil-immersion objectives and a 37°C/5% CO_2 incubation chamber. High-resolution live-cell images (Fig. 1, e and i–j; and Fig. S1) were subject to noise reduction and background subtraction using ImageJ (NIH; http://rsb.info.nih.gov/ij/). Images were merged and assembled in Photoshop (Adobe).

Ribosome isolation and immunoblotting

Ribosomes from ~10^7 Hep2 cells were isolated as previously described (Elkon et al., 1986). Ribosomal subunits were separated by sucrose gradient (10–40%) centrifugation for 16 h at 23,000 rpm in an SW41 rotor (Beckman Coulter). Fractions containing the small and large ribosomal subunits were analyzed by SDS-PAGE, and immunoblots were performed as previously described (Gareiss et al., 2005).

Immunogold electron microscopy

Hep2 cells expressing myc-tagged r-proteins and grown on coverslips were briefly washed in PBS, fixed for 10 min at RT in 2% formaldehyde in PBS (freshly prepared from paraformaldehyde), and washed again in PBS

(3 × 5 min). Free aldehyde groups were quenched by incubation in 50 mM ammonium chloride in PBS for 15 min, followed by PBS wash. For post-embedding labeling, the cells were dehydrated through an ascending ethanol series and infiltrated with LR White (Plano) according to the manufacturer's instructions. Finally, a Beem capsule filled with the unpolymerized resin was invertedly placed on the coverslip. After polymerization at 40°C for 72 h, the glass coverslip was removed and ultrathin sections were cut and placed on nickel grids. For immunolabeling, the sections were washed in PBS and then in PBS containing 0.1% Tween 20 and 1% BSA (PBS1), followed by incubation with anti-myc monoclonal antibody for 1 h at RT at a concentration of 2 μg/ml in PBS1. After several wash steps in PBS1 and PBS2 (PBS containing 0.1% Tween 20 and 0.1% BSA), Nanogold anti-mouse Fab′ conjugates were added for 1 h (Nanoprobes; 1:20 in PBS2). Then, the grids were rinsed with PBS2 and PBS, postfixed with 1.25% glutaraldehyde in PBS for 2 min, and rinsed in distilled water. Finally, the gold particles were silver enhanced using the R-Gent SE-EM kit (Aurion). The sections were rinsed in distilled water and contrasted with uranyl acetate and lead citrate.

For preembedding labeling, the fixed cells were permeabilized for 10 min with 0.05% Triton X-100 in PBS and washed with PBS containing 0.2% BSA (PBS3). Incubation with the first and secondary antibodies was as detailed above except that PBS3 was used throughout. After several wash steps in PBS3 followed by PBS, cells were fixed in 2% glutaraldehyde in PBS (10 min at 4°C), washed in distilled water, and silver enhanced as described. After several wash steps in distilled water, cells were dehydrated and flat embedded in Epon 812 (Serva). Ultrathin sections were stained according to standard methods and examined in an electron microscope (EM10A; Carl Zeiss MicroImaging, Inc.) operating at 80 kV. Endogenous S14, fibrillarin, and RNA polymerase I were localized in Hep2 cells with mAb S14-39, mAb 72B9, and autoimmune serum S18, respectively, following the preembedding labeling protocol outlined above.

Online supplemental material

Fig. S1 shows the localization of IMP3 in the granular compartment of the nucleolus. Online supplemental material is available at http://www.jcb.org/cgi/content/full/jcb.200612048/DC1.

We would like to thank Kathrin Eberhardt, Eva Maria Muth, and Claudia Rohner for technical assistance.

Our work received support from the Deutsche Forschungsgemeinschaft (grant Sche 157/12-3).

Submitted: 8 December 2006
Accepted: 18 April 2007

References

Bernstein, K., J.E. Gallagher, B.M. Mitchell, S. Granneman, and S.J. Baserga. 2004. The small-subunit processome is a ribosome assembly intermediate. *Eukaryot. Cell.* 3:1619–1626.

Chooi, W., and K.R. Leiby. 1981. An electron microscopic method for localization of ribosomal proteins during transcription of ribosomal DNA: a method for studying protein assembly. *Proc. Natl. Acad. Sci. USA.* 78:4823–4827.

de la Cruz, J., D. Kressler, and P. Linder. 2004. Ribosomal subunit assembly. *In* The Nucleolus. M. Olson, editor. Landes Bioscience, New York. 258–285.

Decatur, W., and M.J. Fournier. 2003. RNA-guided nucleotide modification of ribosomal and other RNAs. *J. Biol. Chem.* 278:695–698.

El Hage, A., and D. Tollervey. 2004. A surfeit of factors: why is ribosome assembly so much more complicated in eukaryotes than bacteria? *RNA Biol.* 1:10–15.

Elkon, K., S. Skelly, A. Parnassa, W. Moller, W. Danho, H. Weissbach, and N. Brot. 1986. Identification and chemical synthesis of a ribosomal protein antigenic determinant in systemic lupus erythematosus. *Proc. Natl. Acad. Sci. USA.* 83:7419–7423.

Favaretto, P., A. Bhutkar, and T.F. Smith. 2005. Constraining ribosomal RNA conformational space. *Nucleic Acids Res.* 33:5106–5111.

Fromont-Racine, M., B. Senger, C. Saveanu, and F. Fasiolo. 2003. Ribosome assembly in eukaryotes. *Gene.* 313:17–42.

Gadal, O., D. Strauss, E. Petfalski, P.E. Gleizes, N. Gas, D. Tollervey, and E. Hurt. 2002. Rlp7p is associated with 60S preribosomes, restricted to the granular component of the nucleolus, and required for pre-rRNA processing. *J. Cell Biol.* 157:941–951.

Gareiss, M., K. Eberhardt, E. Krüger, S. Kandert, C. Böhm, H. Zentgraf, C.R. Müller, and M.C. Dabauvalle. 2005. Emerin expression in early development of *Xenopus laevis*. *Eur. J. Cell Biol.* 84:295–309.

Gerbi, S., and A.V. Borovjagin. 2004. Pre-ribosomal RNA processing in multicellular organisms. *In* The Nucleolus. M. Olson, editor. Landes Bioscience, New York. 170–198.

Grandi, P., V. Rybin, J. Bassler, E. Petfalski, D. Strauss, M. Marzioch, T. Schafer, B. Kuster, H. Tschochner, D. Tollervey, et al. 2002. 90S pre-ribosomes include the 35S pre-rRNA, the U3 snoRNP, and 40S subunit processing factors but predominantly lack 60S synthesis factors. *Mol. Cell.* 10:105–115.

Granneman, S., and S.J. Baserga. 2004. Ribosome biogenesis: of knobs and RNA processing. *Exp. Cell Res.* 296:43–50.

Granneman, S., J.E. Gallagher, J. Vogelzangs, W. Horstman, W.J. van Venrooij, S.J. Baserga, and G.J. Pruijn. 2003. The human Imp3 and Imp4 proteins form a ternary complex with hMpp10, which only interacts with the U3 snoRNA in 60-80S ribonucleoprotein complexes. *Nucleic Acids Res.* 31:1877–1887.

Hadjiolov, A. 1985. The Nucleolus and Ribosome Biogenesis. Springer-Verlag Wien, New York. 268 pp.

Hinsby, A., L. Kiemer, E.O. Karlberg, K. Lage, A. Fausboll, A.S. Juncker, J.S. Andersen, M. Mann, and S. Brunak. 2006. A wiring of the human nucleolus. *Mol. Cell.* 22:285–295.

Huang, S. 2002. Building an efficient factory: where is pre-rRNA synthesized in the nucleolus? *J. Cell Biol.* 157:739–741.

Kruiswijk, T., R.J. Planta, and J.M. Krop. 1978. The course of the assembly of ribosomal subunits in yeast. *Biochim. Biophys. Acta.* 517:378–389.

Lazdins, I., M. Delannoy, and B. Sollner-Webb. 1997. Analysis of nucleolar transcription and processing domains and pre-rRNA movements by in situ hybridization. *Chromosoma.* 105:481–495.

Leary, D., M.P. Terns, and S. Huang. 2004. Components of U3 snoRNA-containing complexes shuttle between nuclei and the cytoplasm and differentially localize in nucleoli: implications for assembly and function. *Mol. Biol. Cell.* 15:281–293.

Leung, A., D. Gerlich, G. Miller, C. Lyon, Y.W. Lam, D. Lleres, N. Daigle, J. Zomerdijk, J. Ellenberg, and A.I. Lamond. 2004. Quantitative kinetic analysis of nucleolar breakdown and reassembly during mitosis in live human cells. *J. Cell Biol.* 166:787–800.

Louvet, E., H.R. Junera, S. Le Panse, and D. Hernandez-Verdun. 2005. Dynamics and compartmentation of the nucleolar processing machinery. *Exp. Cell Res.* 304:457–470.

Matera, A., K.T. Tycowski, J.A. Steitz, and D.C. Ward. 1994. Organization of small nucleolar ribonucleoproteins (snoRNPs) by fluorescence in situ hybridization and immunocytochemistry. *Mol. Biol. Cell.* 5:1289–1299.

Meier, U. 2005. The many facets of H/ACA ribonucleoproteins. *Chromosoma.* 114:1–14.

Milkereit, P., H. Kuhn, N. Gas, and H. Tschochner. 2003. The pre-ribosomal network. *Nucleic Acids Res.* 31:799–804.

Nagai, T., K. Ibata, E.S. Park, M. Kubota, K. Mikoshiba, and A. Miyawaki. 2002. A variant of yellow fluorescent protein with fast and efficient maturation for cell-biological applications. *Nat. Biotechnol.* 20:87–90.

Osheim, Y., S.L. French, K.M. Keck, E.A. Champion, K. Spasov, F. Dragon, S.J. Baserga, and A.L. Beyer. 2004. Pre-18S ribosomal RNA is structurally compacted into the SSU processome prior to being cleaved from nascent transcripts in *Saccharomyces cerevisiae*. *Mol. Cell.* 16:943–954.

Pogacic, V., F. Dragon, and W. Filipowicz. 2000. Human H/ACA small nucleolar RNPs and telomerase share evolutionarily conserved proteins NHP2 and NOP10. *Mol. Cell. Biol.* 20:9028–9040.

Puvion-Dutilleul, F., J.P. Bachellerie, and E. Puvion. 1991. Nucleolar organization of HeLa cells as studied by in situ hybridization. *Chromosoma.* 100:395–409.

Puvion-Dutilleul, F., E. Puvion, and J.P. Bachellerie. 1997. Early stages of pre-rRNA formation within the nucleolar ultrastructure of mouse cells studied by in situ hybridization with a 5′ETS leader probe. *Chromosoma.* 105:496–505.

Reimer, G., K.M. Pollard, C.A. Penning, R.L. Ochs, M.A. Lischwe, H. Busch, and E.M. Tan. 1987a. Monoclonal autoantibody from a (New Zealand black × New Zealand white)F1 mouse and some human scleroderma sera target an Mr 34,000 nucleolar protein of the U3 RNP particle. *Arthritis Rheum.* 30:793–800.

Reimer, G., K.M. Rose, U. Scheer, and E.M. Tan. 1987b. Autoantibody to RNA polymerase I in scleroderma sera. *J. Clin. Invest.* 79:65–72.

Royal, A., and R. Simard. 1975. RNA synthesis in the ultrastructural and biochemical components of the nucleolus of Chinese hamster ovary cells. *J. Cell Biol.* 66:577–585.

Thiry, M., T. Cheutin, M.F. O'Donohue, H. Kaplan, and D. Ploton. 2000. Dynamics and three-dimensional localization of ribosomal RNA within the nucleolus. *RNA.* 6:1750–1761.